Chemogenetics Modulation of Electroacupuncture Analgesia in Mice Spared Nerve Injury-Induced Neuropathic Pain through TRPV1 Signalling Pathway

I-Han Hsiao , Chia-Ming Yen , Hsin-Cheng Hsu , Hsien-Yin Liao * , Yi-Wen Lin *

Posted Date: 29 December 2023

doi: 10.20944/preprints202312.2323.v1

Keywords: Neuropathic pain; Chemogenetics; TRPV1; pERK; Electroacupuncture; SSC

Article

Chemogenetics Modulation of Electroacupuncture Analgesia in Mice Spared Nerve Injury-Induced Neuropathic Pain through TRPV1 Signalling Pathway

I-Han Hsiao [1,2], Chia-Ming Yen [3, 4], Hsin-Cheng Hsu [5,6], Hsien-Yin Liao [5,*], Yi-Wen Lin [7] and [8,*]

[1] College of Medicine, School of Medicine, China Medical University, Taichung 40402, Taiwan.
[2] Department of Neurosurgery, China Medical University Hospital, Taichung 40402, Taiwan.
[3] Department of Anesthesiology, Taichung Tzu Chi Hospital, Buddhist Tzu Chi Medical Foundation, Taichung 42743, Taiwan.
[4] School of Post-Baccalaureate Chinese Medicine, Tzu Chi University, Hualien 97004, Taiwan.
[5] College of Chinese Medicine, School of Post-Baccalaureate Chinese Medicine, China Medical University, Taichung 40402, Taiwan.
[6] Department of Traditional Chinese Medicine, China Medical University Hsinchu Hospital, Hsinchu, 302, Taiwan.
[7] College of Chinese Medicine, Graduate Institute of Acupuncture Science, China Medical University, Taichung 40402, Taiwan.
[8] Chinese Medicine Research Center, China Medical University, Taichung 40402, Taiwan.
* Correspondence: jamesliao@mail.cmu.edu.tw (H.-Y.L.); yiwenlin@mail.cmu.edu.tw (Y.-W.L.)

Abstract: Neuropathic pain is initiated by a malfunction of the somatosensory cortex system. Acupuncture had been shown to have therapeutic effects for neuropathic pain, although with uncertain mechanisms. We used electroacupuncture (EA) to treat mice spared nerve injury (SNI) model and explore the underlying molecular mechanisms through novel chemogenetic techniques. Both mechanical and thermal pain were found in SNI mice till four weeks (mechanical: 3.23 ± 0.29 g; thermal: 4.9 ± 0.14 s). Hyperalgesia was attenuated by 2 Hz EA (mechanical: 4.05 ± 0.19 g; thermal: 6.22 ± 0.26 s) but not with sham EA (mechanical: 3.13 ± 0.23 g; thermal: 4.58 ± 0.37 s), suggesting EA's specificity. In addition, animals with transient receptor potential V1 (*Trpv1*) deletion showed no significant induction of neuropathic pain (mechanical: 4.43 ± 0.26 g; thermal: 6.24 ± 0.09 s). Moreover, we found increased levels of inflammatory factors such as interleukin-1 beta (IL1-β), IL-3, IL-6, IL-12, IL-17, tumor necrosis factor alpha, and interferon gamma after SNI modeling, which decreased in EA and *Trpv1*$^{-/-}$ group rather than sham group. Western blot and immunofluorescence analysis showed similar tendency in the dorsal root ganglion, spinal cord dorsal horn, somatosensory cortex (SSC), and anterior cingulate cortex (ACC). In addition, a novel chemogenetics method was used to precisely inhibit SSC to ACC activity showed an analgesic effect through TRPV1 pathway. In summary, our findings indicate a novel mechanism underlying neuropathic pain as beneficial targets for neuropathic pain.

Keywords: neuropathic pain; chemogenetics; TRPV1; pERK; electroacupuncture; SSC

1. Introduction

Pain is a global healthcare concern and the most common reason for people seeking medical intervention. Chronic pain is defined as a continued painful sensation lasting for > 3 months in the clinic and can deteriorate the quality of life. The International Association for the Study of Pain (IASP) categorized chronic pain as primary and secondary pain (1). Primary pain includes fibromyalgia and nonspecific lower back pain (2). Neuropathic pain is one of chronic pain secondary to an underlying syndrome that can arise from nociceptive input even without clear damage or dysfunction (1). Chronic pain is associated with pain signal processing, central sensitization, and neural circuits.

 doi:10.20944/preprints202312.2323.v1

Spontaneous hyperalgesia was frequently detected with unsatisfactory therapy for neuropathic pain. Recent studies show that the central nervous system can suffer alterations in central sensitization in mice (3, 4). Pain continues due to central potentiation, a type of neuronal plasticity, and amplified neural activity after the initiation. Central sensitization also results from inflammation in either peripheral or central nervous system (5).

Neuropathic pain is demarcated as uncomfortable sensation initiated by a malunction of the somatosensory cortex (SSC) induced by central nerve system dysfunction in humans (6). In addition, strokes in the SSC region can also induce neuropathic pain (7). Maladaptive neuroinflammation beyond neuronal damage is the dominant cause of chronic pain, even after stroke resolution. Recently, the microglia has been involved in neuropathic pain as neuroinflammation triggers microglial activation (8). Neuropathic pain is a debilitating condition resulting from central sensitization with increased excitatory inputs from several brain areas, including the SSC, to anterior cingulate cortex (ACC) in response to sensory-discriminative pain features (4). Spared nerve injury (SNI) at sciatica trunk: common peroneal, tibia, or sural nerves, are commonly used to develop animal models for drug developments (9-12)

Transient receptor potential V1 (TRPV1) is a Ca2+ permeable channel associated with pain sensation and inflammation detection (13). TRPV1 is triggered by mechanical force, capsaicin, low pH, or temperatures over 43 °C. TRPV1 was indicated participating in inflammatory, fibromyalgia, and neuropathic pain (14, 15), and is highly expressed in small C-fibers. TRPV1 is significantly increased after both peripheral and central levels such as inflammatory, fibromyalgia, and neuropathic pain models. Trpv1 deletion induced desensitization to thermal stimulation and the inflammatory mediators released from glial cells (4). Moreover, injection of the TRPV1 antagonist reduces thermal pain in mice inflammatory pain. Protease-activated receptor 2 is demonstrated to activate TRPV1 through protein kinase A or C signals (14). HMGB1 was indicated as a nuclear factor enhancing transcription associated with tissue damage, bacterial infection, and inflammation. HMGB1 was known as inflammatory mediators from necrotic or glial cells activated by interleukins (ILs), tumor necrosis factor α (TNF-α), interferon-γ (IFN-γ) (16). HMGB1 can bind to receptor for advanced glycation end-products (RAGE) in regulation of DNA transcription by nuclear factor kappa-light-chain-enhancer of activated B cells (NF-κB). The S100B was a calcium- wrapping proteins, which can bind to RAGE receptor, categorized by the regulation of procedures involved in tissue damage (17).

Acupuncture has been long performed as an alternative cure for pain healing with rare side effects. Recently, electroacupuncture (EA), which provides electric stimulation along with acupuncture for better results and standardization, has been shown to relieve inflammatory, fibromyalgia, and neuropathic pain (18) in several mice models. Moreover, it can alleviate various pain conditions by increasing endogenous opiates (19), and adenosine (20). Moreover, EA was reported to alleviate fibromyalgia pain by attenuating IL-1◉, TNFα, and IFNγ in mice plasma. In addition, we recently showed that EA reliably attenuate either mechanical or thermal hyperalgesia in fibromyalgia mouse models via inhibiting the TRPV1 pathway (4).

In the current research, we hypothesized that neuropathic pain is allied with amplified inflammation and neural hyperactivity from the peripheral dorsal root ganglion (DRG), spinal cord dorsal horn (SCDH), SSC, and ACC. We mimicked neuropathic pain using the SNI mice model and evaluated EA efficacy. Consistent with our hypothesis, EA treatment reduced SNI-induced neuropathic pain which also decreased in *Trpv1*$^{-/-}$ mice. TRPV1 and related factors were significantly amplified in the mice DRG, SCDH, SSC, and ACC regions. Conversely, either EA or Trpv1 gene deletion significantly attenuated this increase. Thus, EA had an anti-nociceptive effect by downregulating TRPV1. Furthermore, we used a novel chemogenetic technique to precisely attenuate hyperactivity in SSC mice. After SSC inhibition, neuropathic pain and TRPV1 signaling were attenuated both in the SSC and ACC. Thus, we provided indication that aforementioned mediators can modify TRPV1 pathway and indicated novel and prospective healing goals for treating neuropathic pain.

 doi:10.20944/preprints202312.2323.v1

2. Materials and Methods

2.1. Animals

All mice conducted here were agreed by the Institute of Animal Care and Use Committee of China Medical University (Permit no. CMUIACUC-2022-408), Taiwan, next the conductor for the use of mice (National Academy Press). Our investigation was designed to include n = 9 (n = 6 for Western blot and n = 3 for immunofluorescence), This study required 45 male C57BL/6 mice including wild type and *Trpv1*$^{-/-}$ mice (Jackson Lab, Bar Harbor, ME) 8–12 weeks' age with body weightiness of 20–25 g. Mice had been kept at a 12-hour dark and light sequence with food and water ad libitum. A model size of 9 mice in each group was essential for ◎ value of 0.05 with power of 80%. The laboratory worker blindly to treatment allocation during analysis and experiment. We alienated the mice into 5 individuals: Normal group (Group 1: Normal) Mice were suffered a skin incision and muscle dissection without nerve incision; Spared nerve incision group (Group 2: SNI): Mice were performed with spared nerve incision; EA group (Group 3: SNI + EA): SNI mice with 2 Hz EA treatment; Sham EA group (Group 4: Sham EA): SNI mice with sham-treatment; *Trpv1*$^{-/-}$ group (Group 5: *Trpv1*$^{-/-}$): *Trpv1* knockout mice with spared nerve incision.

2.2. Neuropathic pain model

We used an SNI model to mimic neuropathic pain in animals (15). Mice were anesthetized with a mixture of Zoletil 50 (50 mg/mL) and Xylazine (10 mg/mL). After shaving the left side thigh and using the femur as a landmark, a linear incision was made along the femoral bone to perform a blunt dissection through the biceps femoris muscle to disclose the three branches of sciatic nerve. The sural nerve, so-called spared nerve, is the thinnest among these branches and needs to be carefully protected. The tibia and common peroneal nerves were split over 2 mm and was removed to induce neural damage and inflammation. In the normal group, only femoris muscle dissection was performed and exposure sciatic nerve and its branches without dissection.

2.3. Electroacupuncture

The 2 Hz EA group received acupuncture on the ST36 of the bilateral leg and electrical stimulation with Trio 300 stimulator (Ito, Japan). The parameters were intensity of 1 mA for 20 min at 2 Hz with a rhythm length of 100 μs, while the sham group only received needle insertion on ST36 without electrical stimulation. ST36 acupoint was selected since it was frequently conducted in traditional Chinese medicine for the handling of numerous categories of pain. Acupuncture needles (1 inch, 36G; YU KUANG, Taiwan) were consensually implanted at a depth of 3-4 mm into the murine ST36 acupoint. Mice ST36 acupoint is positioned roughly 3-4 mm lower and 1-2 mm adjacent to the center of the knee (4). The EA stimulation lasted for two weeks between the third week after SNI surgery and until the end of the fourth week.

2.4. Nociceptive behavioral tests

The hyperalgesic activities were evaluated double per week for four weeks after SNI initiation. The first test was three days after SNI surgery. Animals were transferred to the behavior examination area at room temperature and adjusted to the surroundings for ≥30 min. The animals were stimulated after they calmed down and not sleeping or grooming. In von Frey filament assessment, mice had been positioned at a steel net (75 × 25 × 45 cm) sheltered with a iglass cage (10 × 6 × 11 cm). We used an automated von Frey tester (IITC Life Science Inc., USA) to stimulate each mouse three times with the fiber at hind paw (lesion side) and recorded the force after paw withdrawal. After the mechanical tests, we allowed mice to calm down for ≥ 30 minutes before the Hargreaves' test, for which we used an IITC algesimeter (IITC Life Sciences, SERIES8, Model 390G) to examine thermal hyperalgesia by counting the latency to heat challenge. The mice stood on a panes sheet in a cage under which there was a heater; the emphasis of the prediction bulb was expected exactly at left hind paw. In this test, the thermal hyperalgesic latency was judged by the time of paw removal under heat stimulation (4).

 doi:10.20944/preprints202312.2323.v1

2.5. Western blot analysis

Mice were euthanized with isoflurane and next undergo cervical dislocation. DRG, SCDH, SSC, and ACC proteins had been used to pluck proteins. Proteins were first kept at 4 °C and future stored at –80°C. For protein mining, all contains were standardized in radioimmunoprecipitation (RIPA) lysis solution having 50 mM Tris-HCl, 1 % NP-40, 250 mM NaCl, 50 mM NaF, 5 mM EDTA, 1 mM Na3VO4,0.02% NaN3, and 1× protease inhibitor cocktail (AMRESCO). The mined proteins were run with 8% SDS-Tris glycine gel electrophoresis and relocated to a polyvinylidene difluoride (PVDF) membrane. The membrane was incubated in bovine serum albumin (BSA) in TBS-T buffer (10 mM Tris pH 7.5, 100 mM NaCl, 0.1% Tween 20), followed by incubation with 1st antibody in TBS-T with 1% BSA over 2 hours at refrigerator. Peroxidase-conjugated antibody (1: 5000) was used as suitable secondary antibody. Significant bands were imaginary using an enhanced chemiluminescent tests (PIERCE) via LAS-3000 Fujifilm (Fuji Photo Film Co., Ltd.). The concentration of specific bands in the image was measured with NIH ImageJ (Bethesda, MD, USA). α-tubulin or β-actin were used as an interior control (4).

2.6. Immunofluorescence

After all behavioral tests, mice were euthanized for sample collection by isoflurane inhalants and perfused with 4% paraformaldehyde. The DRG, SC, SSC, and ACC regions were instantly removed and post-fixed with paraformaldehyde at refrigerator for few days. Then, such samples had been transferred to a 30% sucrose solution for cold protection at 4 ºC refrigerator overnight. These fixed tissues were placed in an optimal cutting temperature (OCT) compound and fast freezing through liquid nitrogen and stored at -80ºC. Stored sections were next cut with 20-μm thickness and rapidly engaged on glass slides. The slides were then incubated with paraformaldehyde and nurtured with liquid, consisting of 2% BSA, 0.2% Triton X-100, and 0.03% sodium azide, over 1 h at apartment temperature. Later blocking, the slices were then nurtured with 1st antibody (1:200, Alomone) in a 1% BSA solution at 4 ºC refrigerator. Next, slides were further nurtured with 2nd antibody (1:500) for 2 h at room temperature before fixing with coverslips for imagining under an fluorescent microscope (Olympus, BX-51, Japan).

2.7. Chemogenetic operation

All rodents were anesthetized with isoflurane and next fixed their heads in a stereotaxic device, a 23-gauge, 2 mm stainless cannula was implanted into SSC, 0.5 mm posterior and 1.5 mm lateral of bregma at 175 μm below the cortical superficial and fixed to the skull with dental glue. The injection cannula was implanted and linked with the Hamilton needle via a PE duct to inoculate 0.3 μL of viral liquid more than 3 min through the pump (KD Scientific). Subsequently injection, the shot cannula was preserved at SSC for extra 2 min to permit liquid to diffuse. Next, 0.3 μL of hM4D DREADD (designer receptors exclusively activated by designer drugs: AAV8-hSyn-hM4D(Gi)-mCherry; Addgene Plasmid #50477) were injected into the SSC over two weeks. Clozapine N-oxide (CNO; Sigma C0832) was injected to stimulate the DREADD. CNO was thawed in 5% dimethyl sulfoxide (DMSO; Sigma D2650) and diluted with normal saline before intraperitoneal injection of 1 mg/kg at day 15.

2.8. Statistical analyses

Arithmetical analysis was achieved via SPSS software. All value results were offered as mean ± standard error (SEM). Shapiro-Wilk examination was accomplished to check the normality of obtained results. Statistical consequence among every groups was verified by one-way ANOVA test, surveyed by post hoc Tukey's test. Values of $P < 0.05$ were reflected statistically noteworthy.

 doi:10.20944/preprints202312.2323.v1

3. Results

3.1. Electroacupuncture at mice ST36 acupoint ameliorated mechanical and thermal hyperalgesia in a spared nerve injury-initiated chronic pain model

To understand whether EA can ameliorate neuropathic pain, we used behavioral tests to evaluate treatment efficacy. Before SNI surgery (day 0), all groups presented similar mechanical pain behavior. Three days after SNI, mechanical hyperalgesia was observed in all groups. In addition, all groups except for the *Trpv1*$^{-/-}$ group, became more pain-sensitive over time (Figure 1A, SNI: 3.23 ± 0.29 g, n = 9, *P < 0.05). We did not provide any interventional treatment until 15 days to initiate chronic pain. After the 15th day, 2 Hz EA significantly attenuated mechanical hyperalgesia in the SNI mice model instead of sham group (Figure 1A, EA: 4.05 ± 0.19 g: sham EA: 3.13 ± 0.23 g, n = 9, *P < 0.05). Similarly, lower mechanical nociception was perceived in *Trpv1*$^{-/-}$ mice (Fig.1A, *Trpv1*$^{-/-}$: 4.43 ± 0.26 g, n = 9, *P < 0.05). Thermal hyperalgesia showed a similar tendency. All groups expect *Trpv1*$^{-/-}$ mice, showed a gradual decrease in latency after two weeks (Figure 1B, SNI: 4.9 ± 0.14 s; n = 9, *P < 0.05). After the 15th day, EA significantly reduced thermal hyperalgesia while that in the sham group kept worsening (Figure 1B, EA: 6.22 ± 0.26 s: sham EA: 4.58 ± 0.37 s, n = 9, *P < 0.05). In the thermal pain behavior test, there was no hyperalgesia in *Trpv1*$^{-/-}$ mice from 3rd to 28th day (Figure 1B, *Trpv1*$^{-/-}$, 6.24 ± 0.09 s, n = 9, *P < 0.05). Figure 1C shows a schematic illustration of the SNI procedure.

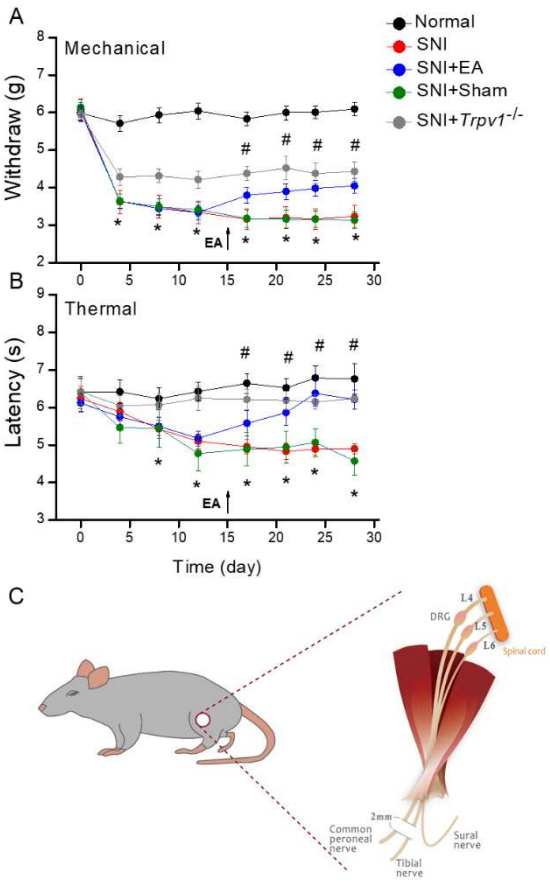

Figure 1. Nociceptor behavior trends. Black: Normal group, red: SNI group, blue: SNI with 2Hz electroacupuncture (SNI + EA) group, green: SNI with Sham group (SNI + Sham EA), and orange: Transient receptor vanilloid member 1 deletion (SNI + *Trpv1*$^{-/-}$) group. From day 0, each node represents post-surgery day 4, 8, 12, 17, 21, 24, 28. *P < 0.05 when compared with the normal group. #P < 0.05 when compared with the SNI group. (A) Mechanical hyperalgesia (von Frey test). (B) Thermal hyperalgesia (Hargreaves' test). (C) Schematic showing the SNI procedure. First, dissecting the muscle and exposing the sciatica nerve with its three branches: common peroneal nerve, tibial

Preprints (www.preprints.org) | NOT PEER-REVIEWED | Posted: 29 December 2023 doi:10.20944/preprints202312.2323.v1

nerve, and sural nerve. Carefully protect and preserve the sural nerve, i.e., spared nerve and cutting another two branches 2 mm at the distal end.

3.2. Electroacupuncture at ST36 restored elevated SNI-derived serum inflammatory mediators

We evaluated the concentration of inflammatory mediators in mouse plasma. SNI mice showed increases of the inflammatory factors such as IL-1β, IL-3, IL-6, IL-12, IL-17, TNF-α, and IFN-γ than normal group (Figure 2, *P < 0.05, n = 9) and similar to sham control (Figure 2, *p < 0.05, n = 9). The intensities of these mediators were lower in the EA and Trpv1 gene deletion groups (Figure 2, EA group: #P < 0.05, n = 9, *Trpv1*$^{-/-}$ group: #P < 0.05, n = 9. In contrast, the cytokine contains were similar in IL-4 and IL-10 levels among groups (Data not shown).

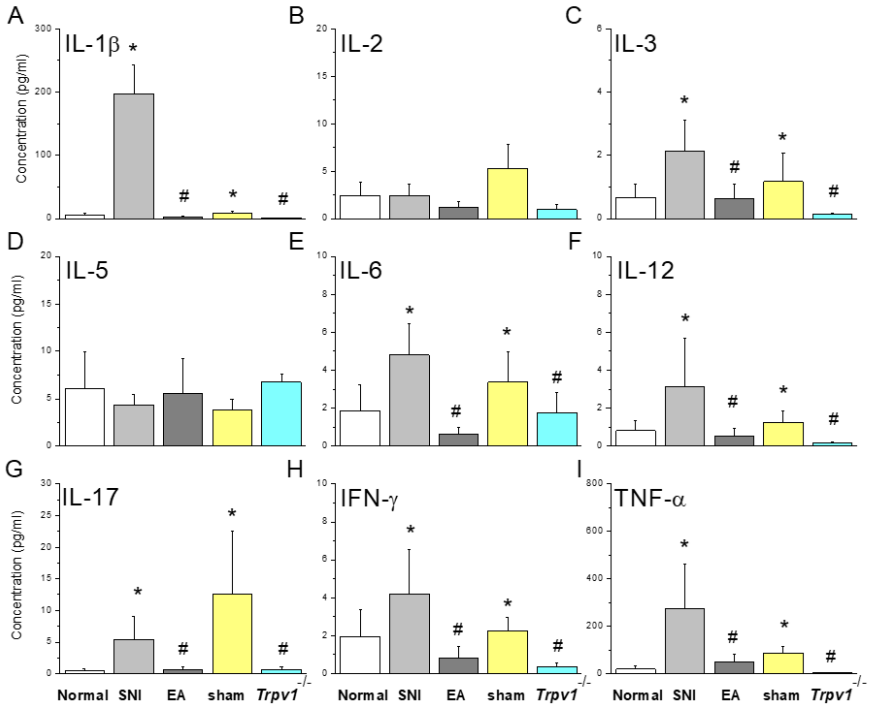

Figure 2. Inflammatory mediators in mice plasma detected by multiplex ELISA. Inflammatory mediators including (A) IL-1β, (B) IL-2, (C) IL-3, (D) IL-5, (E) IL-6, (F) IL-12, (G) IL-17, (H) IFN-γ, and (I) TNF-α. *Indicates statistical significance when compared with the normal group. #indicates statistical significance when compared with the SNI group. IL: Interleukin, IFN: Interferon, TNF: Tumor necrosis factor. n = 9 in all groups.

3.3. Electroacupuncture alleviated the overexpression of microglial transmission and TRPV1-related kinases in mice DRG

Western blot was used to investigate microglial and neuronal markers. SNI mice had higher levels of Iba1, a microglial marker (Figure 3A, *P < 0.05, n = 6). This effect was diminished in the EA and *Trpv1*$^{-/-}$ groups, rather than sham group (Figure 3A, #P < 0.05, n = 6). We next measured HMGB1 and S100B in mice DRG. Similar to Iba1, their expressions were augmented in the SNI group (Figure 3A, *P < 0.05, n = 6) than EA and Trpv1$^{-/-}$ groups (Figure 3A, # P < 0.05, n = 6). The overexpression of HMGB1 or S100B did not alter in sham mice (Figure 3A, *P < 0.05, n = 6). In addition, the SNI group had higher TRPV1 levels (Figure 3A, *P < 0.05, n = 6), but 2 Hz EA meaningfully abridged TRPV1 levels (Figure 3A, #P < 0.05, n = 6). TRPV1 was almost disappeared in *Trpv1*$^{-/-}$ mice. SNI group had increased levels of pPI3K, pAkt, and pmTOR (Figure 3B, *P < 0.05, n = 6) than EA or *Trpv1*$^{-/-}$ mice (Figure 3B, #P < 0.05, n = 6). We also confirmed the involvement of the MAPK pathway by observing higher levels of pERK, pp38, and pJNK in SNI mice (Figure 3B yellow column and 3C black and light gray columns, *P < 0.05, n = 6). Their levels were significantly attenuated in the EA or *Trpv1*$^{-/-}$ groups

Preprints (www.preprints.org) | NOT PEER-REVIEWED | Posted: 29 December 2023 doi:10.20944/preprints202312.2323.v1

compared to the SNI group (Figure 3Byellow column and 3C black and light gray columns, #P < 0.05, n = 6). Furthermore, we observed higher expressions of the transcription factors pNFκB and pCREB in the DRG in the SNI group than in the normal (Figure 3C deep gray and yellow columns, *p < 0.05, n = 6), EA, and *Trpv1*$^{-/-}$ groups (Figure 3C deep gray and yellow columns, #p < 0.05, n = 6). Immunofluorescence staining indicated TRPV1 appearance in the mice DRG. TRPV1 levels significantly increased in the SNI model, an increase attenuated by EA treatment and *Trpv1*$^{-/-}$ mice (Figure 3D, n = 3). Next, immunostaining the DRG with Iba1 an antibody showed higher Iba1 expression in mice DRG of SNI mice then attenuated in EA or *Trpv1*$^{-/-}$ mice (Figure 3E, n = 3). When these two staining images were merged, the SNI and sham groups showed obvious fluorescence compared to control, 2Hz EA and *Trpv1*$^{-/-}$ groups (Figure 3F, n = 3).

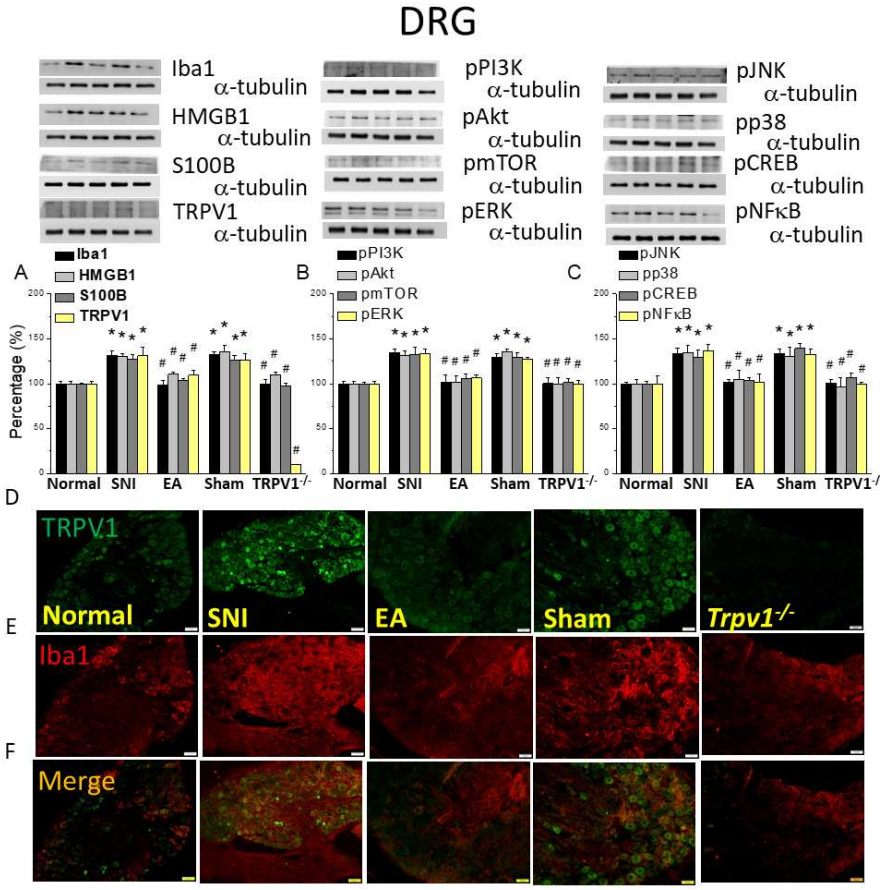

Figure 3. Levels of signaling molecules involved in TRPV1 signaling in the mice DRG. Western blot showing protein expression in the normal, SNI, EA, sham, and *Trpv1*$^{-/-}$ groups. Protein levels of (A) Iba1, HMGB1, S100B, and TRPV1; (B) pPI3K, pAkt, pmTOR pERK; and (C) pJNK, pp38, pCREB, and pNFkB. *p <0.05 compared with the normal group. #p < 0.05 compared with the SNI group. n = 6 in all groups. Immunofluorescence staining of Iba1, TRPV1, and double staining in the mice DRG. (D) Iba1, (E) TRPV1, and (F) Iba1/ TRPV1 double staining, immuno-positive (green, red, or yellow) signals in the mouse DRG. Scale bar: 100 μm. n = 3 in all groups.

3.4. Electroacupuncture alleviated spared nerve injury-induced microglial and TRPV1 increased appearance in the spinal cord dorsal horn

Spinal cord is a main region that conveys pain sensation via dorsal horn being the starting central sensitization. We observed increased expressions of Iba1, HMGB1, S100B, and TRPV1 in the SCDH after SNI (Figure 4A, *P < 0.05, n = 6), which decreased after 2 Hz EA (Figure 4A, #P < 0.05, n = 6). In contrast, sham EA did not change the levels of these proteins. In *Trpv1*$^{-/-}$ mice (Figure 4A), the levels of Iba1, HMGB1, and S100B (Figure 4A, #P < 0.05, n = 6) were significantly lower. EA treatment and *Trpv1* deletion alleviated the intensification in pPI3K-pAkt-pmTOR pathway observed in the SNI

Preprints (www.preprints.org) | NOT PEER-REVIEWED | Posted: 29 December 2023 doi:10.20944/preprints202312.2323.v1

mice (Figure 4B, *P < 0.05, n = 6). In addition, SNI increased pERK, pp38, and pJNK expressions (Figure 4B, *P < 0.05, n = 6), a consequence reversed by EA or Trpv1 deletion (Figure 4B and 4C, #p < 0.05, n = 6). The same tendency was also perceived for pNFκB and pCREB (Figure 4C). Next, immunostaining in the SCDH showed an increase in TRPV1 expression in the SNI group (Figure 4D, n = 3) which 2 Hz EA and *Trpv1*$^{-/-}$ decreased, while the sham group showed similar fluorescence intensity as the SNI group (Figure 4D, n = 3). As shown in Figure 4E (n = 3), we observed a similar pattern for Iba1. We further detected amplified dual staining in the SNI mice SCDH, telling co-localization of TRPV1 and Iba1 (Figure 4F, n = 3). EA or Trpv1 deletion removed aforementioned indications (Figure 4F, n = 3).

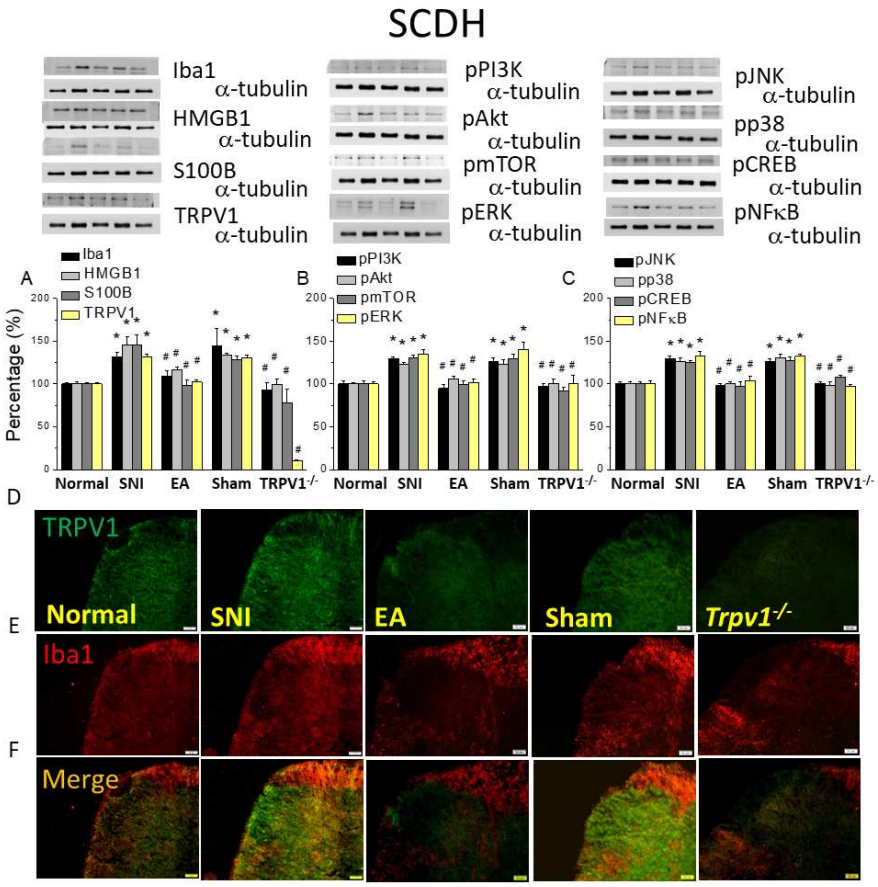

Figure 4. Levels of signaling molecules involved in TRPV1 signaling in the mice SCDH. Western blot protein expression from normal, SNI, 2Hz EA, sham, and *Trpv1*$^{-/-}$ groups. Protein levels of (A) Iba1, HMGB1, S100B, and TRPV1; (B) pPI3K, pAkt, pmTOR pERK; and (C) pJNK, pp38, pCREB, and pNFkB. *p <0.05 compared with the normal group. #p< 0.05 compared with the SNI group. n = 6 in all groups. Immunofluorescence staining of Iba1, TRPV1, and double staining in the mice SCDH. (D) Iba1, (E) TRPV1, and (F) Iba1/ TRPV1 double staining, immuno-positive (green, red, or yellow) signals in the mice SCDH. Scale bar: 100 μm. n = 3 in all groups.

3.5. Electroacupuncture improved microglial hyperfunction and TRPV1 activation in the somatosensory cortex after SNI induction

To determine the microglial or neuronal mechanisms by which TRPV1 modulates SNI-induced neuropathic pain, we detected Iba1 and TRPV1 levels in the mouse SSC. As shown in Figure 5A, the SNI mice had increased Iba1, HMGB1, S100B, and TRPV1 (Fig 5A, *P < 0.05, n = 6) whereas 2 Hz EA downregulated the levels of these four proteins (Figure 5A, #P < 0.05, n = 6). Similar results were observed in the *Trpv1*$^{-/-}$ group instead of sham group. Then, we explored related downstream factors such as pERK, pp38, and pJNK expressions in the cytoplasm and the transcription factors pNFκB and pCREB in the nucleus. All were increased in the SNI group and decreased after 2 Hz EA and Trpv1

Preprints (www.preprints.org) | NOT PEER-REVIEWED | Posted: 29 December 2023 doi:10.20944/preprints202312.2323.v1

deletion. Immunostaining showed similar expression levels for Iba1 (Figure 5D, n = 3) and TRPV1 (Figure 5E, n = 3) in the mice SSC area and increased dual-stained signals in the SNI mice, proposing TRPV1 and Iba1 co-localization (Figure 5F, n = 3), an effect attenuated by EA or Trpv1 deletion, rather than sham EA.

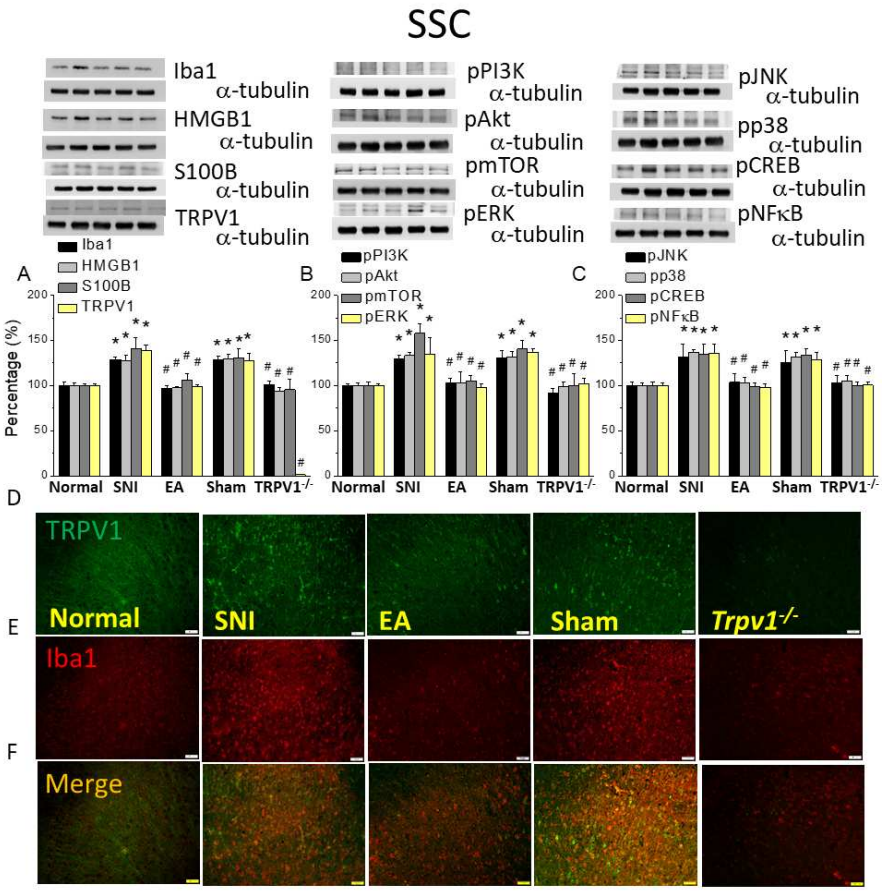

Figure 5. Levels of signaling molecules involved in TRPV1 signaling in the somatosensory cortex (SSC) of the mice. Western blot showing protein expression from normal, SNI, 2Hz EA, sham, and *Trpv1*$^{-/-}$ groups. Protein levels of (A) Iba1, HMGB1, S100B, and TRPV1; (B) pPI3K, pAkt, pmTOR pERK; and (C) pJNK, pp38, pCREB, and pNFkB. *p <0.05 compared with the normal group. #p< 0.05 compared with the SNI group. n = 6 in all groups. Immunofluorescence staining of Iba1, TRPV1, and double staining in the mouse SCC. (D) Iba1, (E) TRPV1, and (F) Iba1/ TRPV1 double staining, immuno-positive (green, red, or yellow) signals in the mice DRG. Scale bar: 100 μm. n = 3 in all groups.

3.6. Electroacupuncture reversed microglial activity, TRPV1 and associated molecules changes in the ACC after SNI

ACC is the terminal region in the pain transmission pathway. As shown in Figure 6A, EA and Trpv1 deletion significantly alleviated the increased Iba1, HMGB1, S100B, and TRPV1 levels after SNI in this region (Figure 6A, *P < 0.05, n = 6). Downstream proteins in mice ACC, such as pPI3K-pAkt-pmTOR, pERK, pJNK, pp38, pNFκB, and pCREB, were all augmented in the SNI group but their levels were restored after 2 Hz EA and Trpv1 loss (Figure 6 B-C, #P < 0.05, n = 6). Immunostaining for Iba1 or TRPV1 in the ACC showed that the SNI group showed higher fluorescence intensity than the control, an effect attenuated by 2 Hz EA and *Trpv1* deletion (Figure 6D-E, n = 3). The sham group presented similar intensity as the SNI group. The merged image showed amplified dual-stained signals in SNI mice and sham group compared to the control, which was diminished by EA or Trpv1 deletion (Figure 6F).

Preprints (www.preprints.org) | NOT PEER-REVIEWED | Posted: 29 December 2023 doi:10.20944/preprints202312.2323.v1

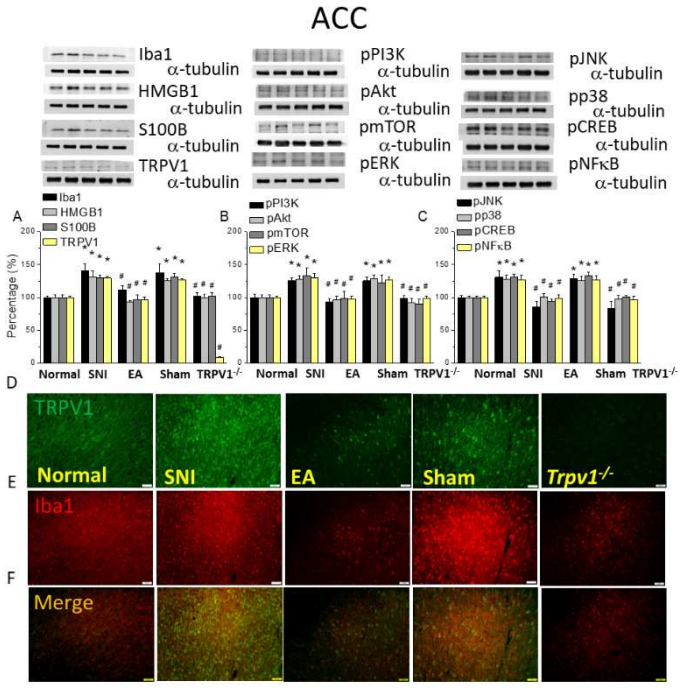

Figure 6. Levels of signaling molecules involved in TRPV1 signaling in the mice ACC. Western blot showing protein expression from normal, SNI, 2Hz EA, sham, and *Trpv1*$^{-/-}$ groups. Protein levels of (A) Iba1, HMGB1, S100B, and TRPV1; (B) pPI3K, pAkt, pmTOR pERK; and (C) pJNK, pp38, pCREB, and pNFkB. *p <0.05 compared with the normal group. #p < 0.05 compared with the SNI group. n = 6 in all groups. Immunofluorescence staining of Iba1, TRPV1, and double staining in the mice DRG. (D) Iba1, (E) TRPV1, and (F) Iba1/ TRPV1 double staining, immuno-positive (green, red, or yellow) signals in the mice DRG. Scale bar: 100 μm. N = 3 in all groups.

3.7. Chemogenetic inhibition of SSC improved neuropathic pain in the mouse SNI model

Figure 7A shows a significant SNI-induced mechanical hyperalgesia from day 0–28 after induction (Figure 7A, black circle, n = 9). In addition, chemogenetic inhibition of the SSC significantly attenuated mechanical hyperalgesia (Figure 7A, red circle, n = 9). With respect to thermal pain, mice under SNI induction showed significant thermal hyperalgesia compared to basal condition (Figure 7B, black circle, n = 9). Furthermore, after CNO injection, thermal hyperalgesia was relieved in mice with SSC inhibition (Figure 7B, red circle, n = 9). Moreover, our data indicated that microglial and TRPV1 associated molecules were not altered in DRG or SCDH of SNI mice and SNI mice subjected to chemogenetic manipulation (Figure 7 C-D, n = 6). In the SSC mice, Iba1, HMGB1, and S100B levels were not altered after CNO injection. Interestingly, TRPV1 and related molecules were attenuated after chemogenetic manipulation (Figure 7E, *P < 0.05, n = 6). A comparable tendency was observed in the mice ACC (Figure 7F, *P < 0.05, n = 6).

Preprints (www.preprints.org) | NOT PEER-REVIEWED | Posted: 29 December 2023 doi:10.20944/preprints202312.2323.v1

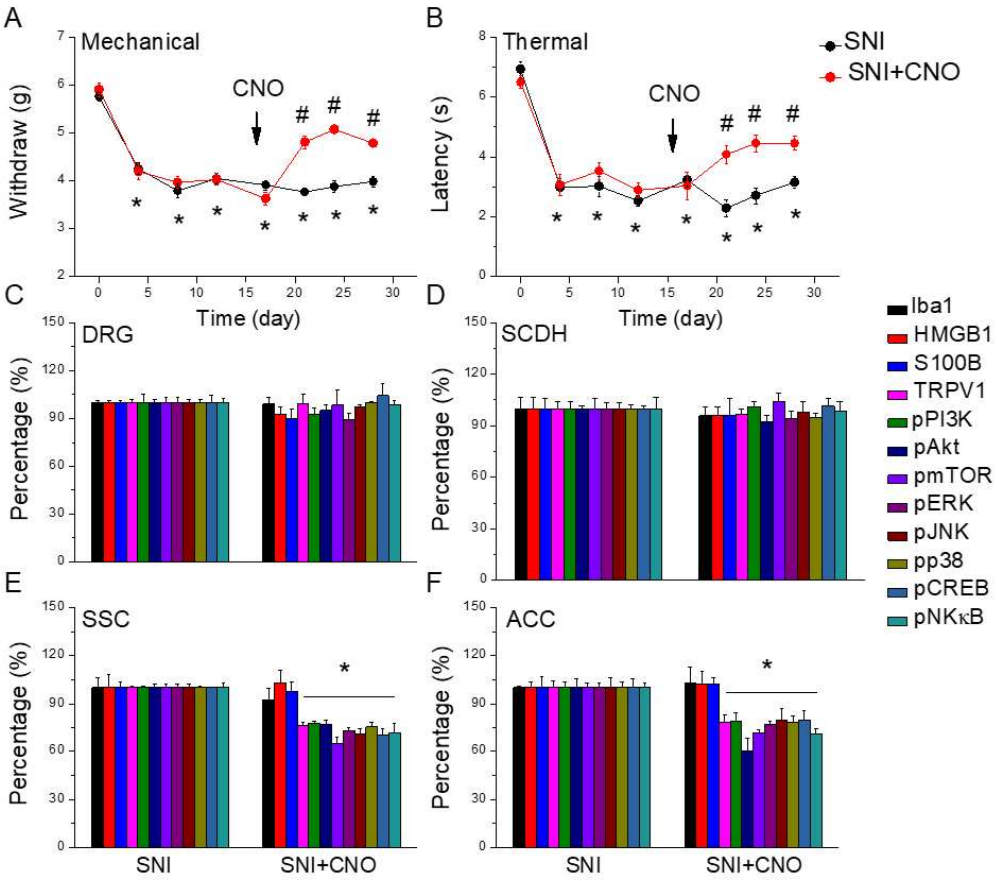

Figure 7. Nociceptor behavior of SNI and SNI animals treated with the chemogenetic technique. Black: SNI group, red: SNI treated with chemogenetics. From day 0, each circle represents post-surgery day 4, 8, 12, 17, 21, 24, 28. * $P < 0.05$ compared with the normal group. # $P < 0.05$ compared with the SNI group. (A) Mechanical hyperalgesia (von Frey test). (B) Thermal hyperalgesia (Hargreaves' test). Protein levels of Iba1, HMGB1, S100B, TRPV1, pPI3K, pAkt, pmTOR, pERK, pJNK, pp38, pCREB, and pNFkB were measured in mice (C) DRG, (D) SCDH, (E) SSC, and (F) ACC.

4. Discussion

When acute nerve damage progresses to a chronic stage, neuropathic pain develops, which gradually deteriorates from nociception to co-morbid emotional and cognitive discomfort (7, 21). Central nervous sensitization, induced by peripheral nerve injury, contributes to chronic neuropathic pain, indicating frequency-dependent increase in hyperexcitability of spinal and brain neuron due to peripheral nerves or tissue injury (21). This sensitization persists via continuous input of a peripheral noxious stimulation signal. Recently, neuroinflammation and associated molecules have been studied to understand neuropathic pain. When the peripheral nerve is damaged, it produces inflammatory stimuli that end up causing neuronal cell death due to oxidative stress. Microglia can secrete MCP-1, IL-1β, IL-6, IL-8, IL-17A, IL-17F, IFN-γ, and TNF-α that interact with each other and with immune T cells (22). Kiguchi et al. reported that IL-1β mRNA in macrophages and Schwann cells were increased in the damaged sciatic nerve by partial sciatic nerve ligation (PSL). Neuropathic pain can be reduced by injection of IL-1β antibody (23). Recent paper indicated that injection of IL-1β and TNF-α at sciatic nerve significantly induced neuropathic pain. Kim and Taylor determined that IL-17 can moderate microglial activation after nerve injury-induced neuropathic pain (24). This combined with immune responses induce unusual synaptic trimming, demyelination, axonal disintegration, regulation of BBB permeability, and immune cell recruitment (5). These mechanisms ultimately result in the suppression of neurogenesis and neuron apoptosis, even neuronal death.

The IASP recommends as effective drugs for neuropathic pain are tricyclic antidepressants, gabapentin, pregabalin, and Duloxetine, Venlafaxine) (25). These oral drugs influence whole -body

 doi:10.20944/preprints202312.2323.v1

synaptic conduction and hence, result in systemic side effects including drowsiness, dizziness, and mouth dryness. A Topical patch with capsaicin is also recommended. For clinical usage, topical capsaicin (8%) patches, applied for 60 min, can inhibit the symptoms for 3 months (26). The mechanism behind capsaicin-based relief from neuropathic pain is associated with the TRPV1 receptor, found on neuronal cell membranes, as capsaicin is a TRPV1 agonist. Theoretically, a high concentration of capsaicin binds to TRPV1 and activates it, opening calcium ion channels leading to a massive influx of calcium ions (27). Then, the neuron degenerate and thus relieve the pain. However, after three months, the neuron regenerate and the pain comes back. However, said treatment methods have many side effects, causing frequent relapses. In comparison, acupuncture is ideal for treating neuropathic pain as it has fewer side effects (28).

In neuropathic pain, neuron and microglia interactions are critical for central sensitization and further developed into chronic pain. However, the association among neurons, microglial, and chronic neuropathic pain remains uncharacterized. Yi et al. reported that microglial inhibition attenuated spinal nerve damage convinced microglial activation and chronic pain. Microglial inhibition also reduced the transcription factor interferon regulatory factor 8 (IRF8) and interleukin 1 beta (IL-1β). They also indicated that reduced microglial function alleviated synaptic transmission following SNT through in vivo spinal cord recording (29). In addition, chemogenetic blockade of the connection of locus coeruleus neuron to the basolateral amygdala decreased chronic pain, anxiety, and enhanced fear learning, whereas its activation dramatically initiated anxiety-aversive learning and memory index (30). Furthermore, CNO administration to mice that had a Gi-DREADD in sensory neuron showed increased latency of paw withdrawal for hot stimuli and indicating an analgesic effect (31). We hence validated that chemogenetic inhibition of the SSC significantly reduced the overexpression of elements in the TRPV1 pathway and down regulated these phenomena in downstream ACC areas. The main limitation of the current research indicated that microglial and TRPV1 signaling pathway were merely perceived in SNI-induced neuropathic pain mice model. Clinical trials are necessary to confirm our present data. We only determine TRPV1 receptor in neuronal level, further study may be focus on other receptors in this model such as TLR2, TLR4, or RAGE receptors (Figure 8). Our data offers evidences of how TRPV1 and associated factors contribute to peripheral and central levels of this neuropathic pain model.

5. Conclusion

In the present study, the behavior test showed increased force in electronic von Frey filament (mechanical pain) and extended latency in the Hargreaves' examination (thermal pain) with 2 Hz EA, showing that it can reverse neuropathic pain similarly to a Trpv1 deletion. Accordingly, we suggest that TRPV1 pathway is crucial in chronic neuropathic pain. Then, we used Western blotting and immunofluorescence to show that 2Hz EA can attenuate microglia and TRPV1 proteins in DRG, SCDH, SSC, and ACC, whereas Trpv1 deletion mice had the same presentation. Furthermore, we detected blood inflammatory factors and observed that EA can inhibit neuroinflammatory factors, i.e. IL-1β, IL-3, IL-6, IL-12, IL-17, IFN-γ, and TNF-α, in the EA i.e. Based on these results, we noted that EA applied to ST36 can attenuate mechanical and thermal hyperalgesia by inhibiting microglia and TRPV1 activity. In summary, we developed an SNI model to mimic neuropathic pain and indicated that EA can attenuate neuropathic pain (Figure 8).

Preprints (www.preprints.org) | NOT PEER-REVIEWED | Posted: 29 December 2023 doi:10.20944/preprints202312.2323.v1

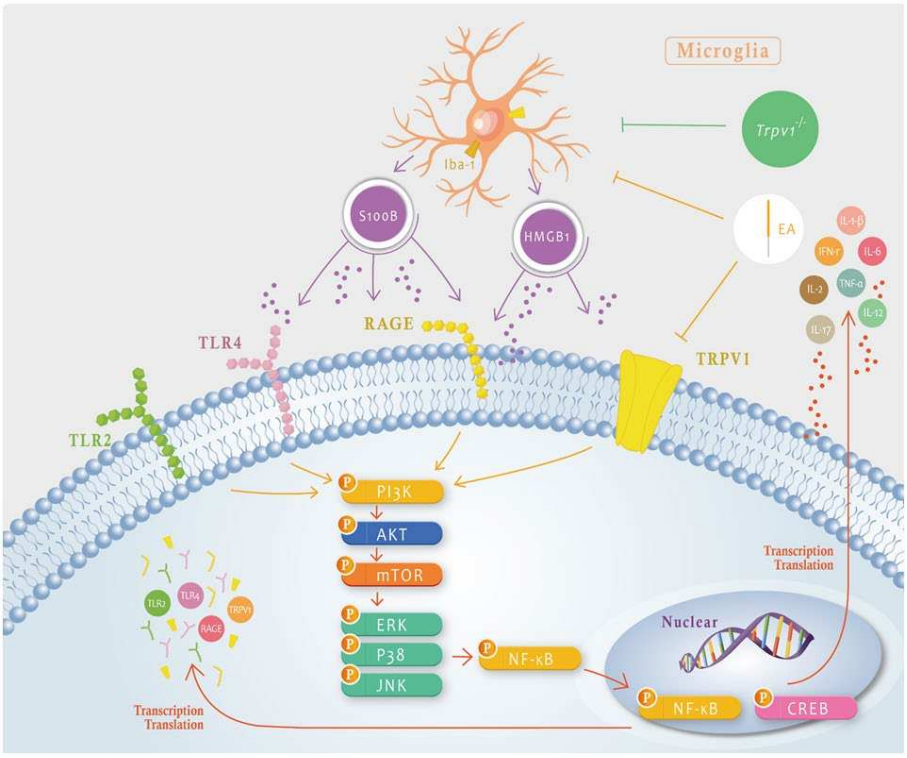

Figure 8. Schematic illustration of the neuron-microglia interaction mechanisms underlying the 2 Hz EA-mediated analgesic effect on SNI-induced neuropathic pain. The summary diagram shows the importance of and mechanisms involving microglia and TRPV1 in neuropathic pain. EA can directly inhibit microglial activity, i.e., Iba1 presentation that will result in HMGB1 and S100B release or directly inhibit TRPV1 on the membrane. *Trpv1*$^{-/-}$ mice have the same phenotype as mice treated with EA.

Author Contributions: HY Liao, IH Hsiao, and CM Yen: Conceptualization, Methodology, Software, Data curation, Writing - original draft, Visualization, Investigation. HC Hsu and YW Lin: Supervision, Validation, Writing - review & editing.

Funding: This work was financially supported by NSTC 112-2314-B-039-021, CMU111-N-28, and the "Chinese Medicine Research Center, China Medical University" from The Featured Areas Research Center Program within the framework of the Higher Education Sprout Project by the Ministry of Education (MOE) in Taiwan.

Data Availability Statement: The datasets supporting the conclusions of this article are included within the article.

Acknowledgments: The authors would like to thank Enago (www.enago.tw) for the English language review.

Conflicts of Interest: There are no financial or other relationships that might lead to a conflict of interest for all authors.

References

1. Raja SN, Carr DB, Cohen M, Finnerup NB, Flor H, Gibson S, et al. The revised International Association for the Study of Pain definition of pain: concepts, challenges, and compromises. Pain 2020; 161 (9): 1976-1982. doi: 10.1097/j.pain.0000000000001939.
2. Baron R, Binder A, Wasner G. Neuropathic pain: diagnosis, pathophysiological mechanisms, and treatment. Lancet Neurol 2010; 9 (8): 807-819. doi: 10.1016/S1474-4422(10)70143-5.
3. Hatch MN, Cushing TR, Carlson GD, Chang EY. Neuropathic pain and SCI: Identification and treatment strategies in the 21st century. J Neurol Sci 2018; 384 75-83. doi: 10.1016/j.jns.2017.11.018.
4. Hsiao IH, Lin YW. Electroacupuncture Reduces Fibromyalgia Pain by Attenuating the HMGB1, S100B, and TRPV1 Signalling Pathways in the Mouse Brain. Evid Based Complement Alternat Med 2022; 2022 2242074. doi: 10.1155/2022/2242074.
5. Malmberg AB, Basbaum AI. Partial sciatic nerve injury in the mouse as a model of neuropathic pain: behavioral and neuroanatomical correlates. Pain 1998; 76 (1-2): 215-222. doi: 10.1016/s0304-3959(98)00045-1.

6. Sarzi-Puttini P, Giorgi V, Marotto D, Atzeni F. Fibromyalgia: an update on clinical characteristics, aetiopathogenesis and treatment. Nat Rev Rheumatol 2020; 16 (11): 645-660. doi: 10.1038/s41584-020-00506-w.
7. Sommer C, Leinders M, Uceyler N. Inflammation in the pathophysiology of neuropathic pain. Pain 2018; 159 (3): 595-602. doi: 10.1097/j.pain.0000000000001122.
8. Yam MF, Loh YC, Tan CS, Khadijah Adam S, Abdul Manan N, Basir R. General Pathways of Pain Sensation and the Major Neurotransmitters Involved in Pain Regulation. Int J Mol Sci 2018; 19 (8): doi: 10.3390/ijms19082164.
9. Yang S, Chang MC. Chronic Pain: Structural and Functional Changes in Brain Structures and Associated Negative Affective States. Int J Mol Sci 2019; 20 (13): doi: 10.3390/ijms20133130.
10. Asgharzade S, Talaei A, Farkhondeh T, Forouzanfar F. A Review on Stem Cell Therapy for Neuropathic Pain. Curr Stem Cell Res Ther 2020; 15 (4): 349-361. doi: 10.2174/1574888X15666200214112908.
11. Forouzanfar F, Tanha NK, Pourbagher-Shahri AM, Mahdianpour S, Esmaeili M, Ghazavi H. Synergistic effect of ellagic acid and gabapentin in a rat model of neuropathic pain. Metab Brain Dis 2023; 38 (4): 1421-1432. doi: 10.1007/s11011-023-01190-x.
12. Rakhshandeh H, Ghorbanzadeh A, Negah SS, Akaberi M, Rashidi R, Forouzanfar F. Pain-relieving effects of Lawsonia inermis on neuropathic pain induced by chronic constriction injury. Metab Brain Dis 2021; 36 (7): 1709-1716. doi: 10.1007/s11011-021-00773-w.
13. Yang C, Yamaki S, Jung T, Kim B, Huyhn R, McKemy DD. Endogenous inflammatory mediators produced by injury activate TRPV1 and TRPA1 nociceptors to induce sexually dimorphic cold pain that is dependent on TRPM8 and GFRalpha3. bioRxiv 2023; doi: 10.1101/2023.01.23.525238.
14. Caterina MJ, Schumacher MA, Tominaga M, Rosen TA, Levine JD, Julius D. The capsaicin receptor: a heat-activated ion channel in the pain pathway. Nature 1997; 389 (6653): 816-824. doi: 10.1038/39807.
15. Cichon J, Sun L, Yang G. Spared Nerve Injury Model of Neuropathic Pain in Mice. Bio Protoc 2018; 8 (6): doi: 10.21769/bioprotoc.2777.
16. Lotze MT, Tracey KJ. High-mobility group box 1 protein (HMGB1): nuclear weapon in the immune arsenal. Nat Rev Immunol 2005; 5 (4): 331-342. doi: 10.1038/nri1594.
17. Leclerc E, Fritz G, Vetter SW, Heizmann CW. Binding of S100 proteins to RAGE: an update. Biochim Biophys Acta 2009; 1793 (6): 993-1007. doi: 10.1016/j.bbamcr.2008.11.016.
18. Yan B, Tang S, Zhang Y, Xiao X. The Role of Glia Underlying Acupuncture Analgesia in Animal Pain Models: A Systematic Review and Meta-Analysis. Pain Med 2023; 24 (1): 11-24. doi: 10.1093/pm/pnac115.
19. Han JS. Acupuncture: neuropeptide release produced by electrical stimulation of different frequencies. Trends Neurosci 2003; 26 (1): 17-22. doi: 10.1016/s0166-2236(02)00006-1.
20. Goldman N, Chen M, Fujita T, Xu Q, Peng W, Liu W, et al. Adenosine A1 receptors mediate local anti-nociceptive effects of acupuncture. Nat Neurosci 2010; 13 (7): 883-888. doi: 10.1038/nn.2562.
21. Herrero JF, Laird JM, Lopez-Garcia JA. Wind-up of spinal cord neurones and pain sensation: much ado about something? Prog Neurobiol 2000; 61 (2): 169-203. doi: 10.1016/s0301-0082(99)00051-9.
22. Zanjani TM, Sabetkasaei M, Mosaffa N, Manaheji H, Labibi F, Farokhi B. Suppression of interleukin-6 by minocycline in a rat model of neuropathic pain. Eur J Pharmacol 2006; 538 (1-3): 66-72. doi: 10.1016/j.ejphar.2006.03.063.
23. Kiguchi N, Maeda T, Kobayashi Y, Fukazawa Y, Kishioka S. Macrophage inflammatory protein-1alpha mediates the development of neuropathic pain following peripheral nerve injury through interleukin-1beta up-regulation. Pain 2010; 149 (2): 305-315. doi: 10.1016/j.pain.2010.02.025.
24. Zelenka M, Schafers M, Sommer C. Intraneural injection of interleukin-1beta and tumor necrosis factor-alpha into rat sciatic nerve at physiological doses induces signs of neuropathic pain. Pain 2005; 116 (3): 257-263. doi: 10.1016/j.pain.2005.04.018.
25. Goh S. Neuropathic pain - definition and drug therapy. Aust Prescr 2018; 41 (6): 178-179. doi: 10.18773/austprescr.2018.069.
26. Baranidharan G, Das S, Bhaskar A. A review of the high-concentration capsaicin patch and experience in its use in the management of neuropathic pain. Ther Adv Neurol Disord 2013; 6 (5): 287-297. doi: 10.1177/1756285613496862.
27. Jones VM, Moore KA, Peterson DM. Capsaicin 8% topical patch (Qutenza)--a review of the evidence. J Pain Palliat Care Pharmacother 2011; 25 (1): 32-41. doi: 10.3109/15360288.2010.547561.
28. Murnion BP. Neuropathic pain: current definition and review of drug treatment. Aust Prescr 2018; 41 (3): 60-63. doi: 10.18773/austprescr.2018.022.
29. Yi MH, Liu YU, Liu K, Chen T, Bosco DB, Zheng J, et al. Chemogenetic manipulation of microglia inhibits neuroinflammation and neuropathic pain in mice. Brain Behav Immun 2021; 92 78-89. doi: 10.1016/j.bbi.2020.11.030.
30. Llorca-Torralba M, Suarez-Pereira I, Bravo L, Camarena-Delgado C, Garcia-Partida JA, Mico JA, et al. Chemogenetic Silencing of the Locus Coeruleus-Basolateral Amygdala Pathway Abolishes Pain-Induced

Anxiety and Enhanced Aversive Learning in Rats. Biol Psychiatry 2019; 85 (12): 1021-1035. doi: 10.1016/j.biopsych.2019.02.018.

31. Saloman JL, Scheff NN, Snyder LM, Ross SE, Davis BM, Gold MS. Gi-DREADD Expression in Peripheral Nerves Produces Ligand-Dependent Analgesia, as well as Ligand-Independent Functional Changes in Sensory Neurons. J Neurosci 2016; 36 (42): 10769-10781. doi: 10.1523/JNEUROSCI.3480-15.2016.